RSC Advances

PAPER

View Article Online
View Journal | View Issue

Cite this: *RSC Adv.*, 2017, **7**, 39127

A novel semi-aromatic polyamide TFC reverse osmosis membrane fabricated from a dendritic molecule of trimesoylamidoamine through a two-step amine-immersion mode†

Hao Wu,‡[ab] Xiao-Lin Chen,‡[ab] Xiang Huang,[ab] Hui-Min Ruan,[ac] Yan-Li Ji,*[ac] Li-Fen Liu *[ac] and Cong-Jie Gao[ac]

In this work, a novel semi-aromatic polyamide RO membrane was fabricated by using a new self-made dendritic molecule trimesoylamidoamine (TMAAM) as a key functional amine monomer that combined 1,3-diamino-2-propanol (DAP) to react with trimesoyl chloride (TMC) through interfacial polymerization technology. By adjusting the TMAAM concentration and amine-immersion mode, this new TMAAM-based semi-aromatic polyamide RO membrane exhibits simultaneously improved water permeability, antifouling and chlorine-tolerant properties. The introduced TMAAM units in polyamide chains can enhance the TMAAM-based membrane's water flux due to its dendritic structure as well as rich hydrophilic groups, and the DAP–TMAAM–TMC membrane prepared *via* the new two-step amine-immersion mode has 1.9 times more water flux without loss of salt rejection than the pristine DAP–TMC membrane and also shows higher water flux than the hand-cast conventional aromatic polyamide MPD–TMC membrane, respectively. At the same time, the regularly distributed hydroxyl groups and aliphatic amide bonds in TMAAM units contribute to the improved hydrophilicity and chlorine-tolerant property of the resultant DAP–TMAAM–TMC membrane, respectively. It is also demonstrated that the new two-step amine-immersion mode leads to a much smoother surface which endows the resultant DAP–TMAAM–TMC membrane with a favorable antifouling ability. This research provides us with a promising functional amine monomer and a new membrane formation method to fabricate a high performance RO membrane.

Received 2nd July 2017
Accepted 30th July 2017

DOI: 10.1039/c7ra07298h

rsc.li/rsc-advances

1. Introduction

Nowadays, reverse osmosis (RO) technology has a wide range of applications in the areas of desalination of seawater and brackish water, production of pure water, concentration of solutions, and wastewater treatment.[1–5] The core of RO technology is the high performance RO membrane, and at present the commercial aromatic polyamide RO membranes used widely in RO process are known for their ideal separation performances including high salt rejection rates and moderate water flux.[6,7] However, these conventional aromatic polyamide materials always suffer from fouling and chlorination during the RO process, which deteriorates the RO membrane's separation performances and shortens its lifetime, and ultimately limits the widespread application of RO technology.[8–13]

Many strategies have been reported to settle the fouling and chlorination problems of RO membranes such as pretreating the RO feed solution, developing new membrane materials, modifying the conventional aromatic polyamide RO membrane and periodic cleaning *etc.*[14–38] However, there are still some limitations such as tedious pretreatment process, complicated modification conditions. Especially, some strategies normally lead to a trade-off effect among the antifouling, chlorine-tolerance and/or reasonable separation performance of the RO membrane, which faces a great challenge to synergistically improve the RO membrane performances.[14,39,40]

It is generally considered that the chlorination of conventional aromatic polyamide results from the *N*-chlorination by attacking of active chlorine and the following benzene ring-chlorination *via* Orton rearrangement, so the aliphatic polyamide structure without aromatic ring has a great potential for improving the chlorine resistance of the RO membrane.[41–43] At the same time, the surface properties including hydrophilicity, morphology, roughness and charge have significant impacts on

[a]*Center for Membrane and Water Science and Technology, Ocean College, Zhejiang University of Technology, Hangzhou 310014, China. E-mail: lifenliu@zjut.edu.cn; yanliji@zjut.edu.cn*

[b]*College of Chemical Engineering, Zhejiang University of Technology, Hangzhou 310014, China*

[c]*Collaborative Innovation Center of Membrane Separation and Water Treatment of Zhejiang Province, Hangzhou 310014, China*

† Electronic supplementary information (ESI) available. See DOI: 10.1039/c7ra07298h

‡ These authors contributed equally.

the antifouling ability of the RO membrane.[6–12] Recently, Hoek *et al.* reported a new polyamide RO membrane with antifouling and chlorine-tolerant properties fabricated from an aliphatic amine of 1,3-diamino-2-propanol (DAP), but this membrane exhibited low water permeability.[44] In the same year, Sum used the dendritic ethylenediamine cored poly(amidoamine) (PAMAM) as a amine monomer to enhance the water permeability of the TFC membrane through interfacial polymerization due to its dendritic and hydrophilic nature, and this membrane presented favorable nanofiltration performance owing to the introduction of the co-polymerized monomer piperazine as a void-filler in the membrane skin layer during interfacial polymerization,[45] which suggested that the dendritic macromolecule has an advantage to improve the membrane water flux due to its large free volume.[46,47] However, to our knowledge, the use of dendritic macromolecule in RO membranes is still quite limited.[48,49]

In this work, a novel dendrimer of trimesoylamidoamine (TMAAM) was designed and synthesized as a key functional amine monomer. Different from the above reported amine monomers, the TMAAM monomer not only exhibits dendritic structure but also contains rich aliphatic amine and hydroxyl groups (Scheme 1), which has some potential advantages for fabrication of the TMAAM-based RO membranes. For example, TMAAM units can enhance the membrane's water permeability due to the existence of hydrophilic groups and its dendritic structure generating more space between polymeric chains. The rich hydrophilic groups in the TMAAM units are also beneficial for the membrane's antifouling. Furthermore, the aliphatic amide structure in polyamide chains contributes to chlorine resistance of the membrane. However, when TMAAM was used as a single amine monomer to react with TMC *via* interfacial polymerization to fabricate the RO membrane, the resulting membrane showed relatively low salt rejection which was also due to the more space between polyamide chains caused by the TMAAM's dendritic structure. Based on above advantages and disadvantages of both dendritic TMAAM and aliphatic amine DAP, therefore, the TMAAM was combined with DAP as the key function monomer in aqueous phase to prepare the novel semi-aromatic polyamide RO membrane with antifouling, chlorine-resistant properties and reasonable separation performance through new interfacial polymerization mode.

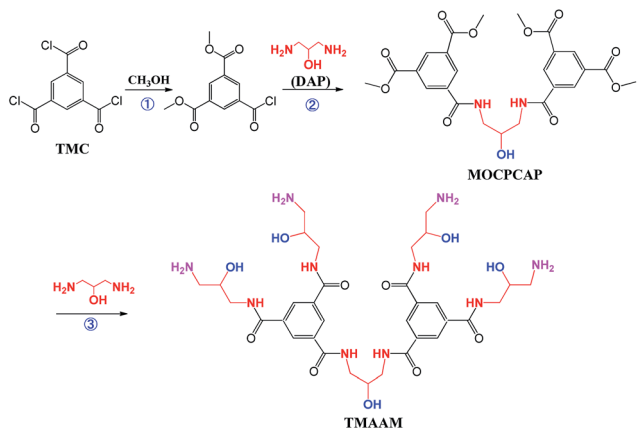

Scheme 1 Synthesis route of trimesoylamidoamine.

2. Experimental section

2.1. Synthesis of the key functional monomer TMAAM

2.1.1. Materials and reagents. Trimesoyl chloride (TMC) and 1,3-diamino-2-propanol (DAP) were purchased from the Shang Hai Bangcheng Co. Ltd., China. Triethylamine (TEA), chloroform, methyl alcohol, ethyl alcohol, DMF were purchased from Aladdin Reagent Co. Ltd (Shanghai, China). All reagents used in monomer synthesis are of analytic grade unless otherwise specified.

2.1.2. Synthesis procedure. The functional monomer trimesoylamidoamine (TMAAM) was synthesized *via* three-step method including esterification, amidation and ester aminolysis reactions (Scheme 1). First, 4.00 g (0.015 mol) TMC was dissolved into 30 ml chloroform in the round-bottom flask and then 1.0 g (0.033 mol) methyl alcohol suspended in 10 ml chloroform was slowly added. The mixture was stirred for a while at room temperature, then heated to 60 °C and refluxed for 4 h. Afterwards the mixture was cooled (2–4 °C cooling bath temperature) and then a solution of 0.69 g (0.0075 mol) DAP, 5.00 g (0.05 mol) TEA in 30 ml chloroform and 1 ml DMF was slowly added in this cooled mixture. After warming up to room temperature, the mixture was stirred to keep reaction for 2.5 h. Following the completion of the reaction, the mixture was washed by 2 × 50 ml water and the resulting organic phase was then dried with sodium sulfate, filtered and concentrated successively. At last, the residue was mixed with 40 g of silica gel and evaporated to dryness and chromatographed with gradient elution (petroleum ether/ethyl acetate 1/1 to ethyl acetate) to obtain 2.30 g white powdery intermediate of 1,3-bis-[3′,5′-bis(methyloxycarbonyl)phenylcarbonylamido]-propane-2-ol (MOCPCAP).

A solution of 2.00 g DAP and 2.10 g MOCPCAP in 60 ml methyl alcohol was added in the round-bottom flask at room temperature and then refluxed for 24 h at 60 °C. After the completion of the reaction, the mixture was transferred from flask into a Rotavapor under vacuum to remove the solvent. Precipitate was get in ethanol, filtered and washed twice with ethanol, and finally dried to get 3.0 g (yield 99%) of a white powdery TMAAM.

2.1.3. Characterization. The product TMAAM was identified by ^{1}H NMR (Brucker-400 M) and ^{13}C NMR (Brucker-400 M), GC-MS (capillary: Trace GC 2000 Series CE Instrument Thermo Quest; MS: Trace C MS Thermo Quest), IR (Nicolet IR200), GC (GC-2010A, Shimadzu Corp., Japan) and melting-point measurement (WRS-1B, Cany instruments Co. Ltd., China).

2.2. Fabrication of TFC reverse osmosis membrane

2.2.1. Materials and reagents. The polysulfone (PSf) microporous supporting film (molecular weight cut-off of about 100 000 g mol^{-1}) was supplied by the Hangzhou Development Center of Water Treatment Technology, China. The key functional monomer TMAAM used to fabricate the RO membrane

was synthesized by ourselves. The other used key monomers include DAP and TMC (Shanghai Bangcheng Co. Ltd., China), *m*-phenylenediamine (MPD) as well as aqueous phase additives including TEA, sodium dodecyl sulfate (SDS) and (+)-10-camphor sulfonic acid (CSA) (J&K Scientific Ltd.). Active chlorine solution used in chlorination experiment was NaClO (Aladdin Reagent Co. Ltd., 5 wt% free chlorine). All other reagents such as *n*-hexane and sodium chloride (NaCl) *etc.* are used as received without further purification unless otherwise specified. Deionized (DI) water ($\leq$5 μS cm^{-1}) was produced by a two-stage reverse osmosis system.

2.2.2. Fabrication of the RO membranes. The new semi-aromatic polyamide TMAAM-based RO membranes were fabricated on the PSf support membrane through interfacial polymerization technology as compared to the pristine DAP-based membrane (DAP–TMC) and conventional aromatic polyamide membrane (MPD–TMC). First, the aqueous solution of MPD (2.0 wt%) or composite amine of DAP and TMAAM (Table 1 and Fig. 1(a)) with TEA (3.0 wt%), SDS (0.15 wt%) and CSA (4.0 wt%) was poured into the top surface of the PSf support membrane (clamped between two Teflon frames) for soaking 2–10 minutes. After removing the excess solution and air-drying until no remaining liquids, the TMC (0.15 wt%) organic phase solution was poured rapidly on the dip-coated surface to react with the adhered amine for 40–60 s, and then the frame with the nascent polyamide skin layer was heated to 60 °C (8–10 min) in the air dryer for further polymerization to obtain the RO membranes including MPD–TMC, DAP–TMC, DAP/TMAAM–TMC and TMAAM–TMC. Finally, the obtained RO membranes were rinsed thoroughly with DI water (conductivity $\leq$ 5 μS cm^{-1}) and stored in $NaHSO_3$ solution (1.0 wt%) for later use.

Since TMAAM molecule is much bigger than DAP molecule, the diffusion speed of TMAAM would be much slower than that of DAP. As compared to the above DAP/TMAAM–TMC membrane prepared *via* conventional single-step amine-immersion mode, the DAP–TMAAM–TMC was fabricated through new two-step

Table 1 Amine composition of the aqueous phase used to prepare the new polyamide membranes

Membrane		Amine composition	Amine-immersion mode
DAP–TMC (M1)	①	2 wt% DAP	Single-step
TMAAM–TMC (M2)	②	2 wt% TMAAM	
DAP/TMAAM–TMC (M3)	③	2 wt% DAP + 0.1 wt% TMAAM	
	④	2 wt% DAP + 0.2 wt% TMAAM	
	⑤	2 wt% DAP + 0.3 wt% TMAAM	
	⑥	2 wt% DAP + 0.4 wt% TMAAM	
	⑦	2 wt% DAP + 0.5 wt% TMAAM	
	⑧	1 wt% DAP + 1 wt% TMAAM	
DAP–TMAAM–TMC (M4)		1 wt% DAP + 1 wt% TMAAM	Two-step

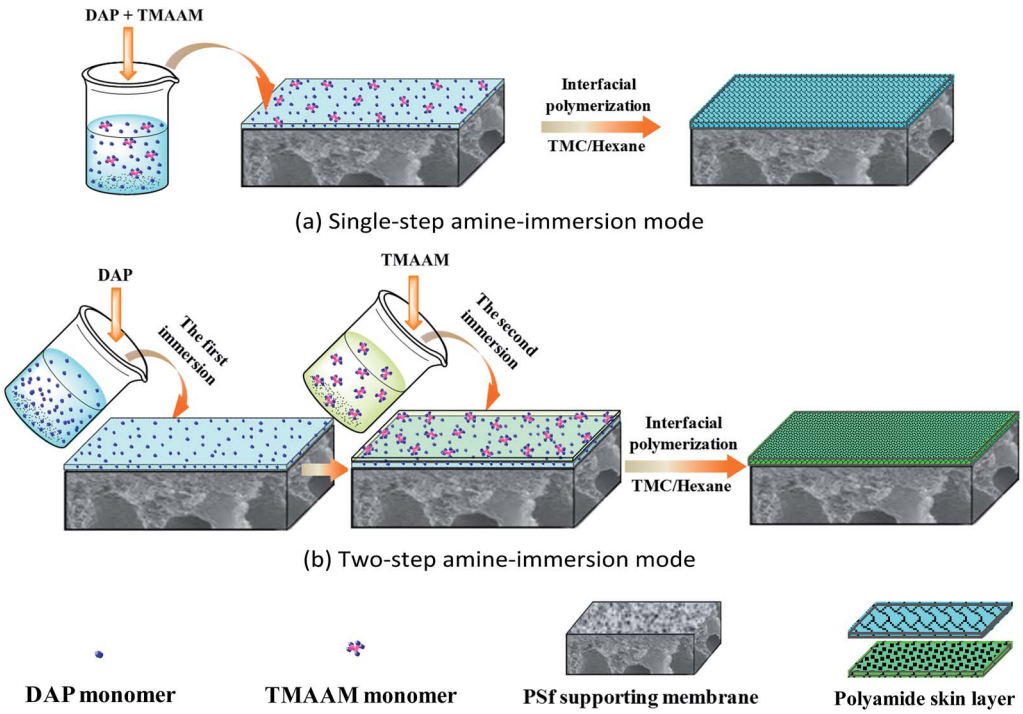

Fig. 1 The amine-immersion modes of RO membrane fabrication.

amine-immersion mode. After the 1 minute immersion of the first aqueous of 1.0 wt% DAP with TEA, SDS and CSA, the second aqueous solution of 1.0 wt% TMAAM with TEA, SDS and CSA was poured on the air-dried DAP-coated surface for 1 minute immersion. Subsequently, the interfacial polymerization reaction with TMC, heat curing and DI water rinse were carried out in a similar manner as mentioned above.

2.3. Membrane separation performance test

The separation performance were tested with cross-flow membrane filtration apparatus (Fig. 2). The membrane coupons (effective area: 12 cm^2) were equilibrated with DI water for at least 30 min (1.55 MPa, 25 °C) before the permeation tests to reach a steady state. Then, permeation tests were carried out with different concentration NaCl solution (pH = 7.0). The experimental data including permeate volume and conductivity (DDS-307, Cany instruments Co. Ltd., China) were recorded after reaching a steady-state flux again. Finally, water flux (J) was calculated from the equation: $J = V/(At)$, where V is the permeate volume, A denotes the effective membrane area, and t is the permeation time. Salt rejection (R) was determined as $R = 1 - C_p/C_f$, where C_p and C_f are permeate and feed concentrations, respectively, which were derived from conductivity analysis.

2.4. Membrane active chlorine exposure experiment

To investigate the membrane's chlorine tolerant property, the membrane coupons were exposed to different concentration chlorine solutions (2000, 6000, 8000 and 10 000 ppm, respectively) for 1 h at room temperature which could effectively simulate long-time exposure to low chlorine concentration, where the active chlorine solutions were prepared with NaClO in DI water at constant pH 8.0. Then, the separation performance of these membranes was tested after being thoroughly rinsed with DI water. Finally, experimental data including water flux and salt rejection were recorded and calculated in a similar manner as above.

2.5. Fouling test

To evaluate the membrane's antifouling property, the dynamic fouling experiment was carried out with a cross-flow membrane filtration apparatus (Fig. 2). In order to avoid the water permeability decline due to compaction, the membrane was pre-pressurized with DI water (1.55 MPa, 25 °C, 2 h) until pure water flux reached a steady state. Then, 10 L of the west lake water with microfiltration pretreatment (Table S1†) was added to the feed tank. After reaching a steady state again (1.55 MPa, 25 °C), the permeation performance of membranes was tested for 8 days. In order to decrease the error of fouling test, 3 samples of the same membrane were loaded in parallel in each fouling test, and the fouling test was also performed for duplicates for 3 times. Finally, the average value was calculated from these experimental data to obtain the variation of water flux and salt rejection of the membranes.

2.6. Characterization of the membranes

Chemical composition and structure of the resultant RO membranes were characterized with attenuated total reflection Fourier transformed infrared spectroscopy (ATR-FTIR, Nicolet6700, Thermo Electron Corporation, USA) and X-ray photoelectronic spectroscopy (XPS, Kratos AXIS Ultra DLD, Shimadzu Corporation, Japan). Surface and cross-section morphologies were observed with scanning electronic microscopy (SEM, S-4700, Hitachi Ltd., Japan) and atomic force microscope (AFM, Park Instrument Auto Probe CT). Static contact angles were obtained with DSA10-MK2 contact angle meter (KRÜSS GmbH Germany). All membrane samples were washed with DI water until no remaining $NaHSO_3$ and dried under vacuum at 40 °C for at least 1 h before measurements.

3. Results and discussion

3.1. Characterization of the chemical structure of TMAAM

The synthetic route for obtaining TMAAM is shown in Scheme 1. As can be seen, TMAAM was prepared *via* three-step method including esterification, amidation and ester aminolysis reactions. The chemical structure of TMAAM were confirmed by FT-IR, ^{13}C NMR, ^{1}H NMR (Scheme 2) and HRMS, and the results are as below.

$C_{33}H_{50}N_{10}O_{11}$ [762.37] mp: 100–103 °C;

IR (KBr): 582.4, 711.1, 961.2, 1048.3, 1096.3, 1291.4, 1432.0, 1542.6, 1651.7, 2930.3, 3077.2 and 3294.6 cm^{-1};

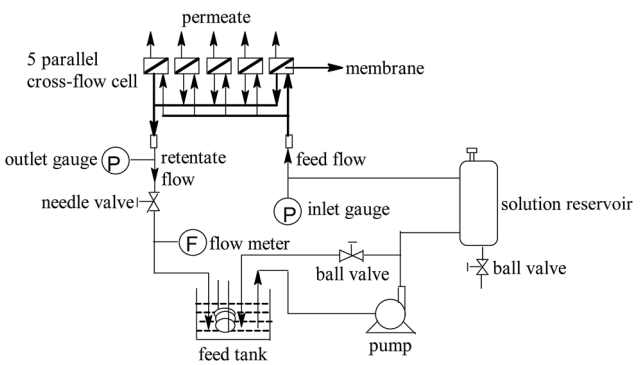

Fig. 2 Device for the permeation tests.

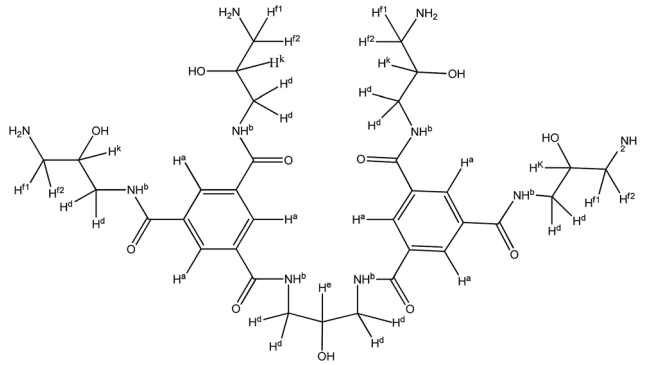

Scheme 2 ^{1}H NMR schematic diagram of TMAAM.

^{1}H NMR (500 MHz, DMSO-d6): δ 8.78–8.66 (m, 6H), 8.46 (t, J = 9.8 Hz, 6H), 3.90 (d, J = 5.3 Hz, 1H), 3.61–3.56 (m, 4H), 3.47–3.42 (m, 12H), 3.36–3.20 (m, 13H), 2.62–2.47 (m, 8H);

^{13}C NMR (126 MHz, DMSO-d6): δ 165.90(2C), 165.84(4C), 135.02(6C), 128.66(6C), 70.79(4C), 68.56, 45.48(6C) and 43.51(4C);

HRMS calculated for $C_{33}H_{51}N_{10}O_{11}$ [M + 1]: 763.3733; found: 763.3717.

3.2. Characterization of the active layer of RO membranes

3.2.1. ATR-FTIR spectrum. ATR-FTIR was used to analyze the chemical structure of the skin layer of RO membranes, as compared IR analyses of the key functional monomers. Fig. 3 presents the main characteristic peaks of the new RO membranes including DAP/TMAAM–TMC and DAP–TMAAM–TMC, compared to the pristine DAP–TMC membrane and the monomers including DAP, TMAAM and TMC. It can be seen that the characteristic peaks of three monomers such as 1760 cm^{-1} (–COCl) and 3294 cm^{-1} (ν N–H, primary amine) disappeared after interfacial polymerization, and new characteristic peaks appeared correspondingly in the ATR-FTIR spectra of membranes. The amide I (ν C=O, 1645, 1649, 1647, 1652 cm^{-1}), II (δ NH, 1502, 1504 cm^{-1}) and III (ν C–N, 1241, 1239, 1240 cm^{-1}) peaks of the active layer respectively are clearly identified as evidence of existing of functional –NHCO– bond. The peaks are located at 1584, 1585 and 1486, 1487 cm^{-1} as expected for the benzene ring vibration. Obviously, the introduction of TMAAM units has few impact on the chemical structure of the polyamide skin layer of the pristine membrane.

3.2.2. XPS analysis of the membranes. XPS is particularly well suited for examining the skin layer of a membrane, because it probes only a short distance (10–90 Å) into the surface of the solid. The quantitative elemental composition of the top-most layer of the sample can be calculated from the spectrum. Therefore, the RO composite membranes with thin active layer (approximately 0.2 μm) were analyzed for the chemical composition of skin layer through XPS analysis.

When polymerizing on the surface of PSf support, it was assumed that two kinds of polymer chains had been formed including DAP–TMC and TMAAM–TMC. The DAP–TMC polymer chain has two possible ideal structures including linear with pendant –COOH (unit A) and totally cross-linked (unit B) as shown in Fig. 4. Since TMAAM was derived from the reaction of DAP and TMC, the totally cross-linked reaction of TMAAM and TMC is similar with that of DAP and TMC. In other words, the TMAAM–TMC polymer chain has the same ideal totally cross-linked structure (unit B), while it has a different linear structure with pendent –COOH (unit C). Herein, the pendant –COOH groups in the linear structures is attributed to the hydrolysis of –COCl groups during interfacial polymerization process. According to these ideal chemical structures, the relative atomic concentration (AC%) of characteristic polyamide elements (C, O and N) and their concentration ratios of the different polymer chains were calculated (Table 2).

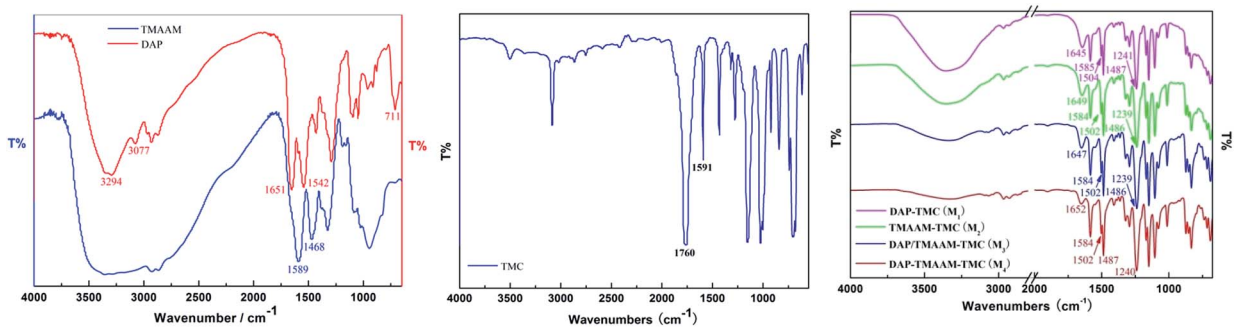

Fig. 3 ATR-FTIR spectrum of TFC RO membranes.

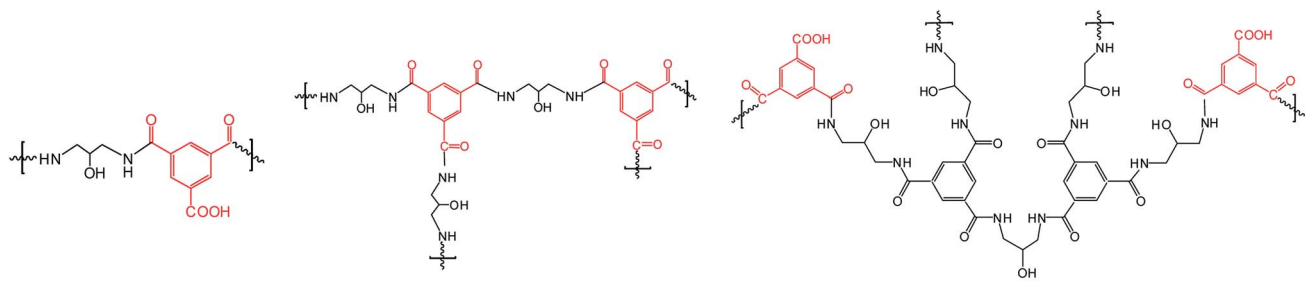

Fig. 4 Possible ideal chemical structures of DAP–TMC and TMAAM–TMC polymer chains.

Table 2 The element composition of RO membranes derived from the XPS measurement

Item			C%	N%	O%	O/N
Calculated data from ideal structures of polymer chains	DAP–TMC	Linear with pendant –COOH (A)	57.14	11.11	31.75	2.85
		Totally cross-linked (B)[a]	58.69	15.22	26.09	1.71
	TMAAM–TMC	Linear with pendant –COOH (C)	57.95	13.26	28.79	2.17
Actual data of XPS analysis of membranes	DAP–TMC (M1)		61.31	11.38	27.31	2.40
	TMAAM–TMC (M2)		61.75	12.07	26.18	2.17
	DAP/TMAAM–TMC (M3)		64.41	10.88	24.70	2.27
	DAP–TMAAM–TMC (M4)		59.77	12.55	27.68	2.21

[a] The TMAAM–TMC polymer chain has the same ideal cross-linked structure of the DAP–TMC polymer chain. Here M3 denotes that the DAP/TMAAM–TMC membrane was fabricated from the no. 8 composite amine as shown in Table 1.

Theoretically, the O atom exists in the pendent –COOH, the cross-linked polyamide bond (–CONH–) and –OH group of DAP monomer, while the N atom is only in the same cross-linked polyamide bond. Obviously, the ratio of O/N is closely related to the cross-linking degree of polymeric structure, and the lower the O/N ratio is, the higher cross-linking degree the RO membrane has. Since the TMAAM monomer was synthesized from a given reaction of TMC and DAP (Scheme 1), TMAAM itself has an exact cross-linking degree and its O/N ratio is 1.1. Whether TMAAM-based polymer chains exhibit linear structure and/or totally cross-linked structure, in other words, their O/N ratios will be lower than 2.85 derived from the ideal linear DAP–TMC structure (unit A) and higher than 1.71 calculated from the ideal totally cross-linked structure (unit B). In fact, it can be seen from the Table 2 that the actual O/N ratio of 2.40 derived from the DAP–TMC membrane is greatly higher than 1.71 from unit B but near 2.85 from unit A, at the same time, it is also higher than 2.17 from unit C as well as greater than all actual O/N ratios of the TMAAM-based RO membranes. These results indicate that the DAP–TMC membrane is mainly composed of the linear DAP–TMC polymer chains and few totally cross-linked structures. It is further noticed that the actual O/N ratio (2.17) of the TMAAM–TMC membrane equals to the ideal value calculated from unit C, in other word, the TMAAM–TMC membrane is just composed of linear structures. However, both the actual O/N ratios of 2.27 from the DAP/TMAAM–TMC membrane and 2.21 from the DAP–TMAAM–TMC membrane are between 2.17 from the TMAAM–TMC membrane and 2.40 from the DAP–TMC membrane, and meanwhile are far from 1.71 calculated from ideal totally cross-linked structure. Obviously, the two membranes of DAP/TMAAM–TMC and DAP–TMAAM–TMC are mainly composed of both linear structures of TMAAM–TMC and DAP–TMC polymer chains, and the DAP–TMAAM–TMC membrane has slightly higher cross-linking degree than the DAP/TMAAM–TMC membrane. The possible reason is that the two-step amine-immersion mode increases the contact chances of TMAAM with TMC which leads to an increase in TMAAM units in the resultant membrane. Furthermore, it should be noticed that all of the three TMAAM-based membranes have higher O/N ratios than the DAP–TMC membrane, in other words, the TMAAM-based membranes have relative higher cross-linking degree due to the introduction of TMAAM units.

3.2.3. Surface morphology of the membranes. The combination of SEM and AFM micrograph was used to observe the surface morphologies of the four new semi-aromatic polyamide RO membranes including DAP–TMC (M1), TMAAM–TMC (M2), DAP/TMAAM–TMC (M3) and DAP–TMAAM–TMC (M4) and the conventional polyamide RO membrane TMC–MPD (M0) (Fig. 5). It can be seen from the SEM images that the four new semi-

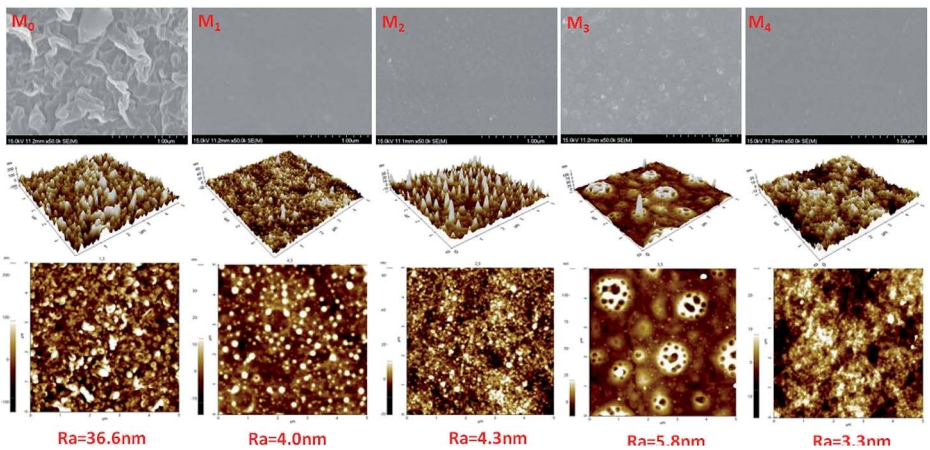

Fig. 5 SEM and AFM images of the RO membranes. M0: MPD–TMC; M1: DAP–TMC; M2: TMAAM–TMC; M3: DAP/TMAAM–TMC; M4: DAP–TMAAM–TMC. Here M3 denotes the DAP/TMAAM–TMC membrane was fabricated from the no. 8 composite amine as shown in Table 1.

aromatic polyamide RO membranes have different surface morphologies from the conventional MPD–TMC membrane and also exhibit much smoother surface. At the same time, the AFM images are in good accord with the SEM images, and the average roughness of all the membranes ranks in the following order: MPD–TMC (36.6 nm) > DAP/TMAAM–TMC (5.8 nm) > TMAAM–TMC (4.3 nm) > DAP–TMC (4.0 nm) > DAP–TMAAM–TMC (3.3 nm), which also demonstrates that the four new semi-aromatic polyamide membranes are very smoother than the conventional full-aromatic polyamide MPD–TMC membrane. Furthermore, it is interesting that a small number of lotus root bulges sporadically distribute on the surface of DAP/TMAAM–TMC membrane prepared *via* conventional single-step amine-immersion mode, which will easily lead to deposition of foulants on the membrane surface, but fortunately the DAP–TMAAM–TMC membrane fabricated *via* the new two-step amine-immersion mode has uniformly smooth surface. Obviously, the two-step amine-immersion mode can improve the surface morphology of the RO membrane. The possible reason is that the large TMAAM molecules dip-coated on the top-most surface of PSf support first contacted and reacted with TMC to form a very loose and rough TMAAM–TMC film due to its dendritic structure generating more space between the polymer chains, and then the small DAP molecules diffused through the resultant nascent TMAAM–TMC film to react with TMC at the interface of two phases and form a smooth DAP–TMC film on the surface of TMAAM–TMC film, as a result of that the DAP–TMAAM–TMC membrane presents smoother surface than the DAP/TMAAM–TMC membrane.

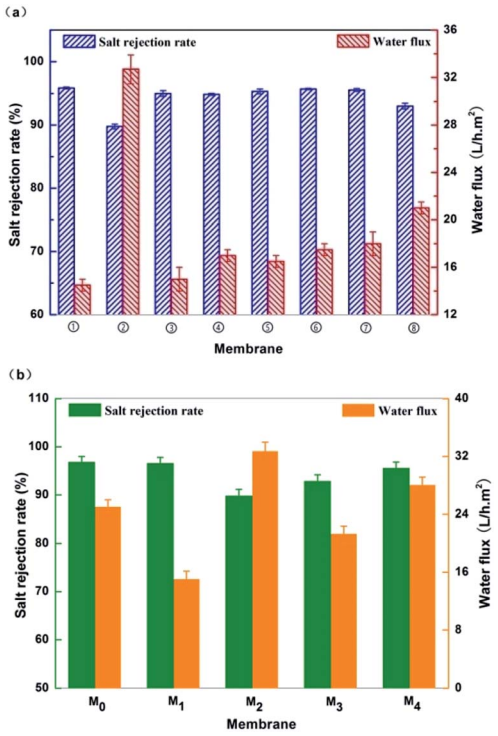

Fig. 6 (a) The impact of different concentration of TMAAM in aqueous phase on the membrane separation performance. (b) Separation performance of the resultant RO membranes. M0: MPD–TMC; M1: DAP–TMC; M2: TMAAM–TMC; M3: DAP/TMAAM–TMC; M4: DAP–TMAAM–TMC. Here M3 denotes the DAP/TMAAM–TMC membrane was fabricated from the no. 8 composite amine as shown in Table 1.

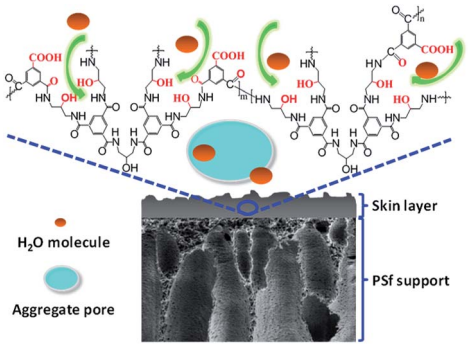

Fig. 7 Schematic illustration of the TMAAM-based polymer chains facilitating the diffusion of water molecules through the RO membrane.

3.3. Separation performance of the membranes

The separation performance of the resultant new semi-aromatic polyamide membranes were tested with 2000 ppm NaCl solution at 1.55 MPa, 25 °C as compared to that of the conventional polyamide MPD–TMC membrane. Fig. 6(a) shows the effects of different concentration of TMAAM in aqueous phase on the water flux and salt rejection rate of the membranes as referred the Table 1. It can be seen that the water flux is increased from 14.5 to 32.7 L h^{-1} m^{-2} with the rise in TMAAM concentration from 0 to 2 wt%, whereas the salt rejection rate of the membranes is correspondingly decreased. Especially, the salt rejection of TMAAM–TMC membrane greatly decreased to 89.8%. Obviously, the addition of TMAAM in the aqueous phase to modify the DAP–TMC membrane can improve the water permeability but simultaneously cause a loss of salt rejection of the membrane. Fortunately, the DAP–TMAAM–TMC membrane prepared *via* new two-step amine-immersion mode has 1.9 and 1.3 times more water flux without loss of salt rejection rate than the DAP–TMC and DAP/TMAAM–TMC membranes respectively as shown in Fig. 6(b).

The possible reason is that the TMAAM molecule not only has a dendritic structure but also contains rich aliphatic amine and hydroxyl groups regularly along with its molecule chain. After membrane formation, the semi-aromatic polyamide chains based on TMAAM dendritic units have rich hydrophilic groups and bonds including –OH, –COOH derived from the hydrolysis of –COCl group and –C=O from the amide bond, which can facilitate water molecules to diffuse through the membrane and thus improve the membrane's water permeability. On the other hand, the TMAAM units lead to more space inside or among the polymer chains, so-called aggregate pore,[47,48] which can not only enhance the water permeability but also reduce the salt selectivity of the membranes (Fig. 7). Therefore, suitable concentration of TMAAM is one of the important factors to get an ideal separation performance of the new TMAAM-based polyamide RO membrane.

3.4. Chlorine-tolerant property of the RO membranes

The chlorination experiments were carried out to evaluate the chlorine-tolerant property of the new semi-aromatic polyamide

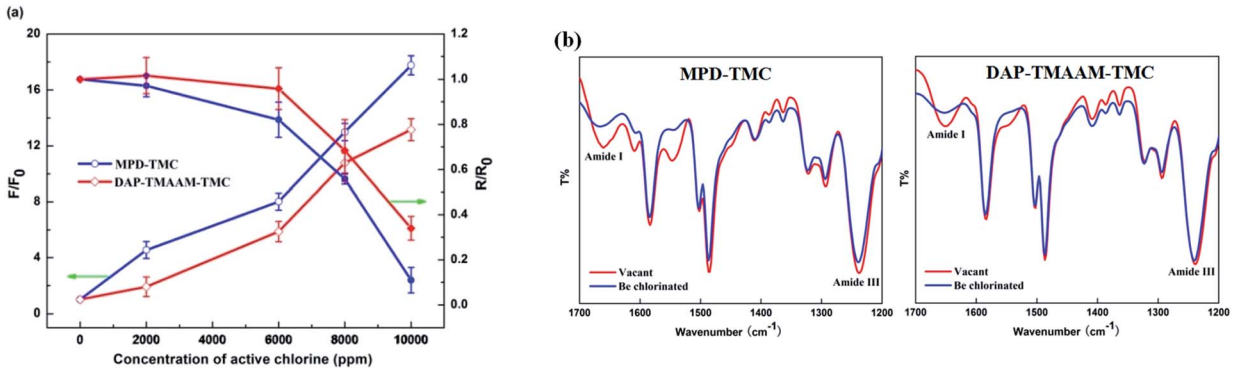

Fig. 8 (a) Separation performance and (b) FTIR variation of the RO membranes after chlorine exposure. (i) MPD–TMC membrane. (ii) DAP–TMAAM–TMC membrane.

Table 3 Variation of O/N ratios of the RO membranes before and after chlorination

Membrane	O/N ratio before chlorination	O/N ratio after chlorination	Difference of O/N ratios	Variation%
MPD–TMC	1.70	2.04	0.74	20
DAP–TMAAM–TMC	2.17	2.35	0.18	8.29

DAP–TMAAM–TMC membrane that has relatively ideal separation performance as demonstrated in above Section 3.3, and compared to that of the conventional polyamide MPD–TMC membrane. It can be seen from the Fig. 8(a) that the chlorine-tolerant property of the DAP–TMAAM–TMC membrane is greatly better than that of the conventional MPD–TMC membrane. At the chlorine concentration less than 2000 ppm h, both of the salt rejection rate and water flux of the DAP–TMAAM–TMC membrane just has a slight increase, while the MPD–TMC membrane exhibits great decrease in both salt rejection rate and water flux. When the concentration of the active chlorine is in the range of 2000 to 6000 ppm h, the salt rejection rate of the DAP–TMAAM–TMC membranes still are kept stable, but the MPD–TMC membrane's salt rejection decreases greatly.

It is well known that the attack of active chlorine will cause a degradation of polyamide chain due to the break of amide bond,[41–43] which mainly presents the variation of amide III (ν C–N) and amide I (ν C=O) peaks in the IR spectrum. As shown in Fig. 8(b), the amide I peaks of the two membranes of DAP–TMAAM–TMC and MPD–TMC present some changes after exposure to 6000 ppm h active chlorine solution. However, the amide III peak of the DAP–TMAAM–TMC membrane just has few changes, while the conventional MPD–TMC membrane exhibits great variation. Meanwhile, the XPS analysis also presents the similar tendency (Fig. S1† and Table 3). The O/N ratios of the skin layer of both MPT–TMC and the DAP–TMAAM–TMC membranes increase with the chlorination, but the difference (0.74) of O/N ratios of the MPD–TMC membrane before and after chlorination is much greater than that of the DAP–TMAAM–TMC membrane (0.18). The possible reason is that the chlorination leads to increase in O element amount which results from the break of amide bond and the formation of new carboxyl group (–COOH) and quinone bond (Ph=O), whereas causes few changes of N element amount unless decrease. On the other hand, since the TMAAM-based semi-aromatic polyamide chains have aliphatic amide bonds, which can avoid benzene ring-chlorination *via* Orton rearrangement and further prevent the

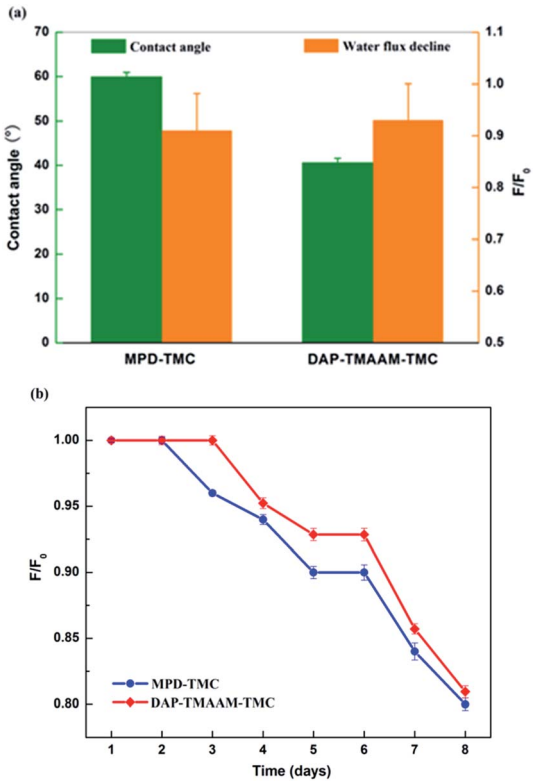

Fig. 9 (a) The contact angle and water flux decline of membranes. (b) The continual fouling test of membranes with west lake water for 8 days.

polyamide chains from break. Obviously, the combination of ATR-FTIR and XPS analyses provides an evidence for the favorable chlorine-tolerant ability of the DAP–TMAAM–TMC membrane.

3.5. Antifouling property of the RO membranes

The contact angle is a measure of the tendency for the water to wet the membrane surface. The lower contact angle means the great tendency for water to wet the membrane and the higher hydrophilicity. As can be seen from the Fig. 9(a), the new semi-aromatic polyamide DAP–TMAAM–TMC membrane has much lower contact angle than the conventional polyamide MPD–TMC membrane, in other words, the former exhibits more hydrophilic surface than the latter. At the same time, the DAP–TMAAM–TMC membrane has lower water flux decline than the MPD–TMC membrane, and the former always shows better antifouling ability than the latter during the continual fouling test as shown in Fig. 9(b). One of the possible reasons is that the DAP–TMAAM–TMC membrane has some –COOH groups as well as a large number of –OH groups derived from the TMAAM units as confirmed by the above XPS analysis. The other reason is probably attributed to the much smooth surface as demonstrated by the above AFM measurement. Obviously, the much hydrophilic and smooth surface of the DAP–TMAAM–TMC membrane greatly contribute to its favorable antifouling property due to the introduction of the TMAAM units in the polyamide skin layer *via* the new two-step amine-immersion mode.

4. Conclusions

A novel semi-aromatic polyamide TFC RO membrane was fabricated by using the new self-made dendritic molecule of TMAAM through the new two-step amine-immersion mode. Due to the introduction of TMAAM unites in polyamide chains, the resultant DAP–TMAAM–TMC membrane exhibits simultaneously improved water flux without loss of salt rejection, antifouling and chlorine-tolerant properties compared to the pristine DAP–TMC membrane and the hand-cast conventional polyamide MPD–TMC membrane. The introduced TMAAM units can facilitate water molecules to diffuse through the RO membrane and enhance the membrane's water flux due to its dendritic structure as well as rich hydrophilic groups. At the same time, the regularly distributed hydroxyl groups and aliphatic amide bonds in the TMAAM units can improve the hydrophilicity and chlorine-tolerant property of the resultant semi-aromatic polyamide DAP–TMAAM–TMC membrane, respectively. Moreover, the two-step amine-immersion mode leads to smooth surface of the DAP–TMAAM–TMC membrane, which thus endows this membrane with favorable antifouling ability.

Acknowledgements

Financial support is acknowledged to the National Basic Research Program of China (No. 2015CB655303), Zhejiang Provincial Natural Science Foundation of China (No. LY13B060006) and the Open Research Fund Program of Collaborative Innovation Center of Membrane Separation and Water Treatment of Zhejiang Province.

Notes and references

1 M. A. Shannon, P. W. Bohn, M. Elimelech, J. G. Georgiadis, B. J. Marinas and A. M. Mayes, Science and technology for water purification in the coming decades, *Nature*, 2008, **452**(7185), 301–310.
2 M. Elimelech and W. A. Phillip, The Future of Seawater Desalination: Energy, Technology, and the Environment, *Science*, 2011, **333**, 712–717.
3 K. P. Lee, T. C. Arnot and D. Mattia, A review of reverse osmosis membrane materials for desalination—Development to date and future potential, *J. Membr. Sci.*, 2011, **370**, 1–22.
4 S. S. Shenvi, A. M. Isloor and A. F. Ismail, A review on RO membrane technology: Developments and challenges, *Desalination*, 2015, **368**, 10–26.
5 W. J. Lau, S. Gray, T. Matsuura, D. Emadzadeh, J. Paul Chen and A. F. Ismail, A review on polyamide thin film nanocomposite (TFN) membranes: History, applications, challenges and approaches, *Water Res.*, 2015, **80**, 306–324.
6 G.-R. Xu, J.-N. Wang and C.-J. Li, Polyamide nanofilm composite membranes (NCMs) supported by chitosan coated electrospun nanofibrous membranes: Preparation and separation performance research, *Desalination*, 2013, **328**, 31–41.
7 T. Fujioka, N. Oshima, R. Suzuki, W. E. Price and L. D. Nghiem, Probing the internal structure of reverse osmosis membranes by positron annihilation spectroscopy: Gaining more insight into the transport of water and sma, *J. Membr. Sci.*, 2015, **486**, 106–118.
8 Y.-N. Kwon and J. O. Leckie, Hypochlorite degradation of crosslinked polyamide membranes: II. Changes in hydrogen bonding behavior and performance, *J. Membr. Sci.*, 2006, **282**, 456–464.
9 G.-D. Kang, C.-J. Gao, W.-D. Chen, X.-M. Jie, Y.-M. Cao and Q. Yuan, Study on hypochlorite degradation of aromatic polyamide reverse osmosis membrane, *J. Membr. Sci.*, 2007, **300**, 165–171.
10 G.-d. Kang and Y.-m. Cao, Development of antifouling reverse osmosis membranes for water treatment: A review, *Water Res.*, 2012, **46**, 584–600.
11 D. Rana and T. Matsuura, Surface modifications for antifouling membranes, *Chem. Rev.*, 2010, **110**, 2448–2471.
12 L. Zhao, P. C. Y. Chang, C. Yen and W. S. W. Ho, Dow Chemical: Materials Science Contributions to Membrane Production, *J. Membr. Sci.*, 2013, **425–426**, 1.
13 H. C. Yang, J. Hou, V. Chen and Z. K. Xu, Surface and interface engineering for organic-inorganic composite membranes, *J. Mater. Chem. A*, 2016, **4**, 9716–9729.
14 L. Henthome and B. Boysen, State-of-the-art of reverse osmosis desalination pretreatment, *Desalination*, 2015, **356**, 129–139.
15 D. Saeki, H. Karkhanechi, H. Matsuura and H. Matsuyama, Effect of operating conditions on biofouling in reverse osmosis membrane processes: Bacterial adhesion, biofilm

formation, and permeate flux decrease, *Desalination*, 2016, **378**, 74–79.

16 L.-F. Liu, S.-C. Yu, Y. Zhou and C.-J. Gao, Study on a novel polyamide-urea reverse osmosis composite membrane (ICIC-MPD) I. Preparation and characterization of ICIC-MPD membrane, *J. Membr. Sci.*, 2006, **281**, 88–94.

17 L.-F. Liu, S.-C. Yu, L.-G. Wu and C.-J. Gao, Study on a novel polyamide-urea reverse osmosis composite membrane (ICIC-MPD) II. Analysis of membrane antifouling performance, *J. Membr. Sci.*, 2006, **283**, 133–146.

18 H. D. Raval, J. J. Trivedi, S. V. Joshi and C. V. Devmurari, Flux enhancement of thin film composite RO membrane by controlled chlorine treatment, *Desalination*, 2010, **250**, 945–949.

19 A. C. Sagle, E. M. V. Wangner, H. Ju, B. D. McCloskey, B. D. Freeman and M. M. Shama, PEG-coated reverse osmosis membranes: Desalination properties and fouling resistance, *J. Membr. Sci.*, 2009, **340**(1), 92–108.

20 J. A. Blok, R. Chhasatia, J. Dilag and V. A. Ellis, Surface initiated polydopamine grafted poly([2-(methacryoyloxy) ethyl]trimethylammonium chloride) coatings to produce reverse osmosis desalination membranes, *J. Membr. Sci.*, 2014, **468**, 216–223.

21 Y. Hu, K. Lu, F. Yan, S. Yu, Y. Shi, P. Yu, S. Li and C. Gao, Enhancing the performance of aromatic polyamide reverse osmosis membrane by surface modification via covalent attachment of polyvinyl alcohol (PVA), *J. Membr. Sci.*, 2016, **501**, 209–219.

22 Q. Zhang, C. Zhang, J. Xu, Y. Nie, S. Li and S. Zhang, Effect of poly(vinyl alcohol) coating process conditions on the properties and performance of polyamide reverse osmosis membranes, *Desalination*, 2016, **379**, 42–52.

23 J. Xu, Z. Wang, J. Wang and S. Wang, Positively charged aromatic polyamide reverse osmosis membrane with high anti-fouling property prepared by polyethylenimine grafting, *Desalination*, 2015, **365**, 398–406.

24 M. S. Rahaman, H. Therien-Aubin, M. Ben-Sasson, C. Ober, B. Nielsena and M. Elimelech, Control of biofouling on reverse osmosis polyamide membranes modified with biocidal nanoparticles and antifouling polymer brushes, *J. Mater. Chem. B*, 2014, **2**, 313–316.

25 J. Q. Meng, Z. Cao, L. Ni, Y. Zhang, X. Wang, X. Zhang and E. Liu, A novel salt-responsive TFC RO membrane having superior antifouling and easy-cleaning properties, *J. Membr. Sci.*, 2014, **461**, 123–129.

26 J. Wang, Z. Wang, J. Wang and S. Wang, Improving the water flux and bio-fouling resistance of reverse osmosis (RO) membrane through surface modification by zwitterionic polymer, *J. Membr. Sci.*, 2015, **493**, 188–199.

27 J. Wu, Z. Wang, Y. Wang, W. Yan, J. Wang and S. Wang, Improving the hydrophilicity and fouling resistance of RO membranes by surface immobilization of PVP based on a metal-polyphenol precursor layer, *J. Membr. Sci.*, 2015, **495**, 58–69.

28 H. J. Kim, K. Choi, Y. Baek, D. G. Kim, J. Shim, J. Yoon and J. C. Lee, High-Performance Reverse Osmosis CNT/Polyamide Nanocomposite Membrane by Controlled Interfacial Interactions Mater, *ACS Appl. Mater. Interfaces*, 2014, **6**(4), 2819–2829.

29 W. F. Chan, H. Y. Chen, A. Surapathi, M. Taylor, X. Shao, E. Marand and J. Johnson, Zwitterion Functionalized Carbon Nanotube/Polyamide Nanocomposite Membranes for Water Desalination, *ACS Nano*, 2013, **7**(6), 5308–5319.

30 S. Inukai, R. Cruz-Silva, J. Ortiz-Mddina, M.-G. Aaron, K. Takeuchi, T. Hayashi, A. Tanioka, T. Araki, T. Tejima, T. Noguchi, M. Terrones and M. Endo, High-performance multifunctional reverse osmosis membranes obtained by carbon nanotube polyamide nanocomposite membrane, *Sci. Rep.*, 2015, **5**, 13562.

31 Y. K. Kim, S. Y. Lee, D. H. Kim, *et al.*, Preparation and characterization of thermally crosslinked chlorine resistant thin film composite polyamide membranes for reverse osmosis, *Desalination*, 2010, **250**, 865–867.

32 X. Wei, Z. Wang, J. Chen, *et al.*, A novel method of surface modification on thin-film-composite reverse osmosis membrane by grafting hydantoin derivative, *J. Membr. Sci.*, 2010, **346**, 152–162.

33 J. Xu, X. Feng and C. Gao, Surface modification of thin-film-composite polyamide membranes for improved reverse osmosis performance, *J. Membr. Sci.*, 2011, **370**, 116–123.

34 C. Wang, G. K. Such, A. Widjays, *et al.*, Click poly(ethylene glycol) multilayers on RO membranes: Fouling reduction and membrane characterization, *J. Membr. Sci.*, 2012, **409–410**, 9–15.

35 L.-F. Liu, D.-Z. Xu, H.-L. Chen and C.-J. Gao, Preparation and Characterization of a Novel Polyimide-urethane Reverse Osmosis Composite Membrane Material, *J. Chem. Eng.*, 2012, **33**, 1605–1612.

36 J. Xu, Z. Wang, L. Yu, J. Wang, *et al.*, A novel reverse osmosis membrane with regenerable anti-biofouling and chlorine resistant properties, *J. Membr. Sci.*, 2013, **435**, 80–91.

37 L.-F. Liu, Z.-B. Cai, J.-N. Shen, L.-X. Wu, E. M. V. Hoek and C.-J. Gao, Fabrication and characterization of a novel poly(amide-urethane@imide) TFC reverse osmosis membrane with chlorine-tolerant property, *J. Membr. Sci.*, 2014, **469**, 397–409.

38 Y.-L. Ji, Q.-F. An, Y.-S. Guo, W.-S. Hung, K.-R. Lee and C.-J. Gao, Bio-inspired fabrication of high perm-selectivity and anti-fouling membranes based on zwitterionic polyelectrolyte nanoparticles, *J. Mater. Chem. A*, 2016, **4**, 4224–4231.

39 B. Penate and L. Garcia-Rodriguez, Seawater reverse osmosis desalination driven by a solar Organic Rankine Cycle: Design and technology assessment for medium capacity range, *Desalination*, 2012, **284**, 86–91.

40 S. S. Shenvi, A. M. Isloor and A. Ismail, A review on RO membrane technology: Developments and challenges, *Desalination*, 2015, **368**, 10–26.

41 T. Kawaguchi and H. Tamura, Chlorine-resistant membrane for reverse osmosis. II. Preparation of chlorine-resistant polyamide composite membranes, *J. Appl. Polym. Sci.*, 1984, **29**, 3369–3379.

42 J. Koo, R. J. Peterson and J. E. Cadotte, ESCA Characterization of Chlorine-Damaged Polyamide Reverse Osmosis Membrane, *ACS Polym. Prepr.*, 1986, **27**, 391.

43 K. Nita, Y. Matsui, S. Konagaya and M. Miyagi, in *ICOM'90*, Chicago, 1990, p. 1055.

44 E. M. V. Hoek and B. Feingerg, Chlorine-tolerant polyamide derivatives for preparing biofouling-resistant reverse osmosis membranes and membranes made there from WO 2014107523 A2, *US Pat.*, PCT/US2014/010091, 2014.

45 J. Y. Sum, A. L. Ahmad and B. S. Ooi, Synthesis of thin film composite membrane using mixed dendritic poly(amidoamine) and void filling piperazine monomers, *J. Membr. Sci.*, 2014, **466**, 183–191.

46 A. Sarkar, P. I. Carver, T. Zhang, A. Merrington, K. J. Bruza, J. L. Rousseau, S. E. Keinath and P. R. Dvornic, Dendrimer-based coatings for surface modification of polyamide reverse osmosis membranes, *J. Membr. Sci.*, 2010, **349**, 421–428.

47 L. Lianchao, W. Baoguo, T. Huimin, C. Tianlu and X. Jiping, A novel nanofiltration membrane prepared with PAMAM and TMC by in situ interfacial polymerization on PEK-C ultrafiltration membrane, *J. Membr. Sci.*, 2006, **269**, 84–93.

48 Y. Zhou, W. Huang, J. Liu, X. Zhu and D. Yan, Self-assembly of hyperbranched polymers and its biomedical applications, *Adv. Mater.*, 2010, **22**, 4567–4590.

49 W. Jiang, Y. Zhou and D. Yan, Hyperbranched polymer vesicles: from self-assembly, characterization, mechanisms, and properties to applications, *Chem. Soc. Rev.*, 2015, **44**, 3874–3889.